SAND87-2365
Unlimited Release
Printed December 1987

Distribution
UC-94E

3-D Finite Element Calculation of Subsidence Induced Deformation of the Weeks Island Service Shaft

Dale S. Preece
Advanced Technology Division
Sandia National Laboratories
Albuquerque, New Mexico 87185

Abstract

The Service Shaft at the Weeks Island SPR facility has experienced vertical and lateral movement since it was constructed in 1905. Movement of the shaft over the past few years has been confirmed through survey levels of the shaft collar and two plumbline surveys of the top 100 feet of the shaft. This 3-D finite element calculation was done to gain an understanding of the deformation of the Service Shaft due to the subsidence of the surrounding material. Subsidence at the site results from creep closure of the bi-level room-and-pillar salt mine which is currently the reservoir for 73 million-barrels of crude oil. The 3-D finite element model treats the southwest corner of the mine and contains 118 pillars on two levels of the mine. The deformation of the Service Shaft is determined from the displacement of a vertical line of nodes in the model which is assumed to be the axis of the Service Shaft. The calculation shows that the Service Shaft is tilting to the northeast and moving downward. The movement, however, is mostly a rigid body rotation and translation with very slight bending and stretching of the shaft. Because the bending and tensile strains are insignificant, this calculation indicates that rupture of the shaft is unlikely.

Contents

Figures

Tables

1. Introduction

The Weeks Island Salt Dome is located south of New Iberia, Louisiana in the south central part of the state and along the coast. The island, which rises 170 feet above the surrounding marshland, is approximately two miles in diameter. Two site characterization studies have been performed and contain important geotechnical details about the island (Acres International, 1977 and 1986).

Rock salt mining production began in 1902 when the Service Shaft was constructed. With its completion, mining of a room-and-pillar mine commenced on what is now termed the upper level. The floor of this level is at approximately -535 msl (feet below Mean Sea Level). Mining on the lower level, which has a floor elevation of approximately -735 msl, began in 1955.

The U. S. Department of Energy purchased these two mine levels and the space directly above them for the U. S. Strategic Petroleum Reserve (SPR) program in 1975. The two levels of rooms and pillars were modified for oil storage by constructing bulkheads at all entrances and constructing drawdown pumping facilities and access drifts in the salt above the oil storage area. The pumping facility at the site resides in the Manifold Room which was constructed in the Service Shaft by increasing its diameter. In late 1979 and early 1980 the facility was filled with 73 million barrels (MMbbl) of crude oil. The two oil storage levels along with the Service and Production Shafts are shown schematically in Figure 1.1.

Two-dimensional finite element calculations addressing the structural stability of the two oil storage levels were performed as part of the initial geotechnical investigations (Hilton et al, 1979) (Acres International, 1977). Two-dimensional calculations were also performed to determine the safe spacing between the lower storage level and a proposed Morton mine below the oil storage area (Preece and Krieg, 1984). However, due to the 3-D nature of the room-and-pillar mine and the lack of a 3-D computational creep capability, 3-D structural stability or subsidence calculations were not performed until now.

In the present study a 3-D finite element model has been created to represent the southwest corner of the mine. The model was designed so that the Service Shaft would be close to the center of the model. It has 118 pillars on two levels of the mine. The Service Shaft is not included as a structural entity in the model but is assumed to follow the movement of the rock and soil. Deformation of the Service Shaft is therefore determined from the displacement of a line of nodes representing

the axis of the shaft. The calculation covers the years 1905 through 2030. Mining of the lower level is simulated using the element death option and oil fill is simulated with pressure boundary conditions on the walls of the rooms.

This study is motivated by the fact that rupture of the Service Shaft would likely result in flooding of the underground facilities including the pumps in the Manifold Room. Flooding would result because the Service Shaft passes through a layer of gravel, sand and clay which contains an almost infinite supply of water and has high permeability (Acres International, 1986). Flooding of the Manifold Room would result in loss of drawdown capability for a significant period of time while a new pumping facility was constructed on the surface.

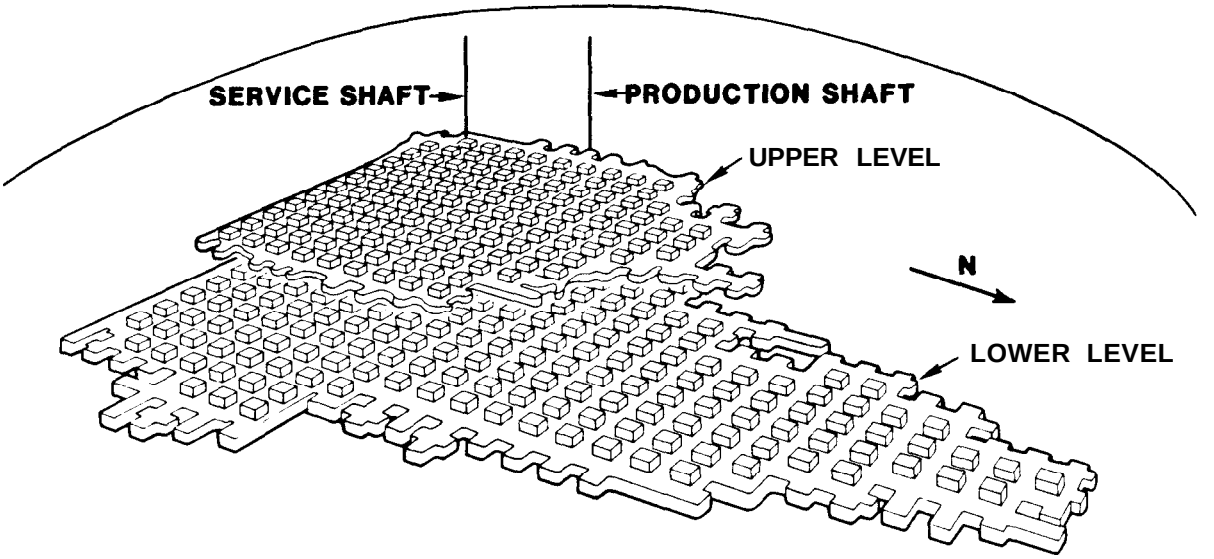

Figure 1.1. Schematic Drawing of the Two SPR levels at Weeks Island Showing the Location of the Service and Production Shafts

2. Finite Element Computer Programs

JAC3D (Biffle, 1986) is a finite element computer program developed for efficient nonlinear analysis of three-dimensional solids. It employs the conjugate gradient iterative technique to obtain a solution. Spatial integration is performed using a single Gauss point in each eight node hexahedral element. An hourglass viscosity technique is used to control the zero energy modes that occur with single point integration. The single point integration combined with the explicit nature of the program and exploitation of CRAY-XMP computer architecture results in very efficient execution. This has made 3-D creep analyses possible on real configurations. Several examples of previous 3-D creep calculations performed with this program are documented in Preece and Sutherland, 1986; Preece, 1986; and Arguello, Munson and Preece, 1987.

The implementation of the secondary creep formulation is described by Krieg, 1983. This creep formulation is not restricted to JAC and JAC3D but has been used in other finite element programs (Stone et al, 1985).

3. Material Properties For Rock Salt and Overburden

Salt core from Weeks Island has been tested quasi-statically for strength and elastic constants (Hansen, 1977) but documentation of any creep testing has not been found. The elastic constants for West Hackberry and Weeks Island are similar enough that they could be used interchangeably in a calculation without causing a significant difference in the results. Even though creep properties vary from site to site it has been shown that the variance from one site to another is usually within the data scatter at any particular site (Herrmann and Lauson, 1981). Thus, the creep model parameters derived from extensive triaxial creep testing of West Hackberry salt have been used in this study (Wawersik and Zeuch, 1984). The secondary creep model is implemented in the finite element program by expressing the creep strain rate magnitude, $\dot{\bar{e}}$, as a function of effective stress, $\bar{\sigma}$

$$\dot{\bar{e}} = D exp\left(\frac{-Q}{RT}\right)\bar{\sigma}^{n} \qquad (3.1)$$

where D and n are constants and Q is an activation energy $\left(\frac{cal}{mole}\right)$, R is the universal gas constant (1.987 $\frac{cal}{mole\ K}$) and T is the material temperature (K). The laboratory determined creep coefficients for West Hackberry salt are given in Table 3.1 along with the elastic constants.

Table 3.1. West Hackberry Secondary Creep Formulation

$D = 1.453\text{-}30 \ \frac{1}{(day)(psf)^n}$
$Q = 12.0 \ \frac{kcal}{mole}$
$n = 4.73$
Young's Modulus = 5.1E7 psf
Poisson's Ratio = 0.30

The magnitude of the creep strain rate, $\dot{\bar{e}}$, and the effective stress, $\bar{\sigma}$, can be calculated from the creep strain rate tensor, $\dot{\mathbf{e}}^{c}$, and the deviatoric stress tensor, $\boldsymbol{\sigma}'$,

respectively as follows.

$$\dot{\bar{e}} = \sqrt{\frac{2}{3}\dot{\mathbf{e}}^c\dot{\mathbf{e}}^c} \tag{3.2}$$

$$\bar{\sigma} = \sqrt{\frac{3}{2}\boldsymbol{\sigma}'\boldsymbol{\sigma}'} \tag{3.3}$$

The flow rule relating the creep strain rate tensor is related to the deviatoric stress tensor by

$$\dot{\mathbf{e}}^c = |\dot{\mathbf{e}}^c|\frac{\boldsymbol{\sigma}'}{|\boldsymbol{\sigma}'|} \tag{3.4}$$

The components of the total strain rate tensor, $\dot{e}_{ij}$, are obtained by summing the components of creep strain rate tensor, $\dot{e}^c_{ij}$, along with the components of the bulk, elastic and thermal strain rate tensors as follows.

$$\dot{e}_{ij} = \dot{e}^c_{ij} + \frac{\nu}{E}\dot{\sigma}_{kk}\delta_{ij} + \frac{1+\nu}{E}\dot{\sigma}_{ij} + \alpha\dot{T}\delta_{ij} \tag{3.5}$$

Where σ_{ij} are the components of the stress tensor, ν is Poisson's ratio, E is Young's modulus, T is absolute temperature, α is the coefficient of linear thermal expansion, δ_{ij} is the Kronecker Delta. A constant temperature of 300K was assumed for these calculations.

A few references documenting finite element calculations that have employed this secondary creep formulation are: (Krieg et al, 1981), (Branstetter and Preece, 1983), (Preece and Wawersik, 1984), (Morgan et al, 1985) and (Morgan et al, 1986).

The above constitutive model includes only secondary creep which is one of the simplest creep models and has some limitations. The same formulation with the same parameters was used to calculate the closure of the South Drift of the WIPP. Calculated South Drift closures differed from measured closures by a factor of approximately three (Morgan et al, 1985 and 1986). For WIPP excavations, dividing Young's modulus by 12.5 was found to be a simple, but not necessarily physically meaningful, method for bringing the calculated closures into agreement with measured closures (Morgan et al, 1987). The same simple method has been applied in this study and the Young's modulus shown in Table 3.1 is the measured value for West Hackberry (and also Weeks Island) Salt divided by 12.5.

The material above the salt has been characterized as a sandy gravel with some clay lenses. In this study the sandy gravel was treated as an elastic material since the deviatoric stresses and strains in the layer never become significant enough to demand a more sophisticated constitutive model. Young's modulus was determined from laboratory testing of the sandy gravel to be 9.0E5 psf (Acres International, 1986) and Poisson's ratio was assumed to be 0.25 based on judgement.

4. 3-D Finite Element Model

4.1 Model Geometry

The geometry of the model is an approximation of the actual geometry at the site. Even though it is an approximation, it is the most accurate and sophisticated finite element model ever made of the Weeks Island mine or probably any other mine. The entire model, which contains 21780 nodal points and 18916 finite elements, is shown in Figure 4.1. The Service Shaft is not represented as a structural entity in the model but is assumed to follow the deformations of the surrounding material. The axis of the Service Shaft is assumed to be a vertical line of nodes in the model, the displacement of which is assumed to be the displacement of the Service Shaft. The location of the top of the shaft at the ground surface is shown in Figure 4.1. The depth of the interface between the salt and the sandy gravel was made as close as possible to the actual depths at the four corners of the model and at the service shaft (Acres International, 1986).

Figure 4.2 shows the finite element model after it has been sectioned and material removed for viewing the inside of the model. As the north arrow indicates, north corresponds to the Y axis and east corresponds to the X axis. The model has 64 pillars on the lower level and 54 pillars on the upper level of the mine. Each pillar in the model is 100 feet square, 75 feet high and is divided into eight finite elements. The rooms between pillars are 50 feet wide and the rooms on the lower level are initially (1905) unmined. The finite elements constituting the material in the lower level rooms are all removed in 1955 to simulate mining of that level. Removal of the material on the lower layer can be seen in Figures 5.3 and 5.4 which are color stress plots that will be discussed in the next section. The southwest corner of the lower level extends out from under the upper level by a few pillars. This was simulated in the model by the lack of rooms in the southwest corner of the upper level.

4.2 Finite Element Mesh Generation

PATRAN (PDA Engineering, 1987), a 3-D mesh generator, was used to create this model. The model was created by first generating the geometry for a single pillar in the southwest corner of the lower level. This pillar was then copied and translated eight times in the X direction to create the row of pillars on the south side of the lower level. This row of pillars was then copied and translated eight times in the Y direction to create the 64 pillars on the lower level. The 64 pillars making up the

lower level were then copied and translated in the *Z* direction to make 64 pillars on the upper level. The rooms between pillars in part of southwest corner of the upper level were then filled. The geometry between, above and below the layers was then defined and the entire model was filled with nodal points and finite elements.

4.3 Boundary Conditions and Loading

Symmetry boundary conditions were applied to the four vertical faces of the model and the bottom. This means that the displacements on each face with symmetry boundary conditions are constrained perpendicular to the face but are unconstrained in the plane of the face. The model was also subjected to gravity loading and the initial stress in each element throughout the model was set to lithostatic.

4.4 Time History

The time history treated in the calculation is an approximation to that which actually occured. The time history assumed in the calculation is shown in Table 4.1.

Table 4.1. Time History Assumed for the Numerical Simulation

Year	Event
1905	Entire Upper Level Opened Instantly
1955	Entire Lower Level Opened Instantly
1980	Oil Fill Occurs Instantly
2030	End of Calculation

The approximation to reality occurs because the upper and lower layers were not mined instantly but slowly over long periods of time. Also, the oil fill did not occur instantly but took many months to complete. Implementing a mining sequence in the model is possible but seems to be an unnecessary increase in sophistication, especially since we do not know the actual mining sequence. The oil fill in the

model was simulated by applying pressure to the roof, walls and floors of the mine in 1980. The pressure was determined from the elevation difference between a particular pressure surface (roof, wall or floor) and the upper level of the oil in the mine which was assumed to be -470 msl.

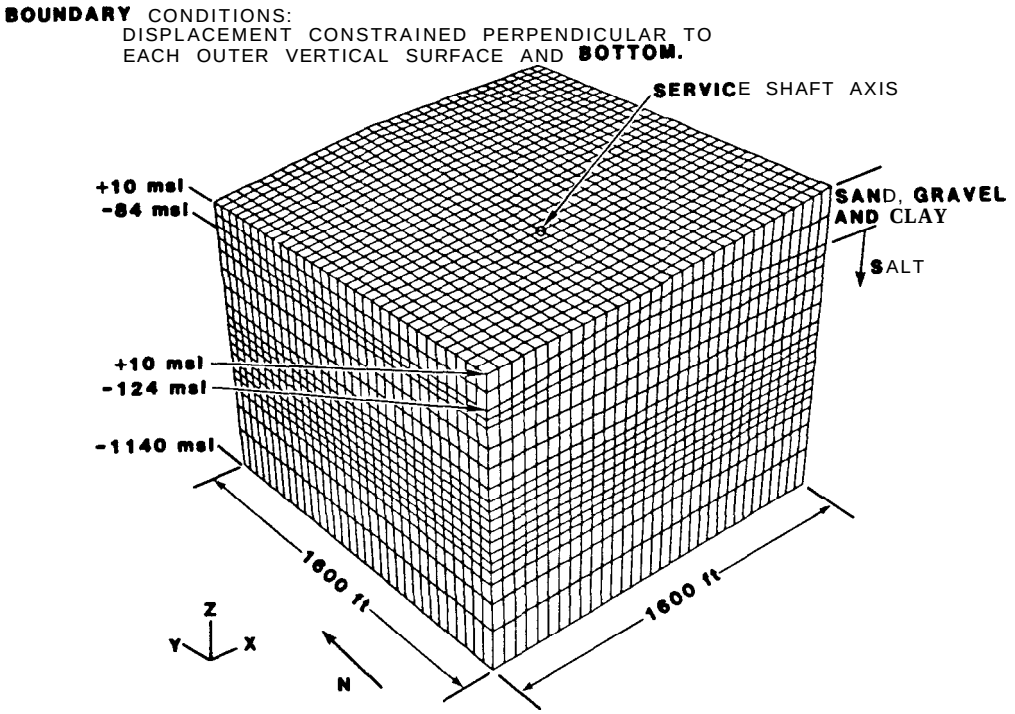

Figure 4.1. 3-D Finite Element Model for Calculation of Subsidence Induced Movement of the Weeks Island Service Shaft.

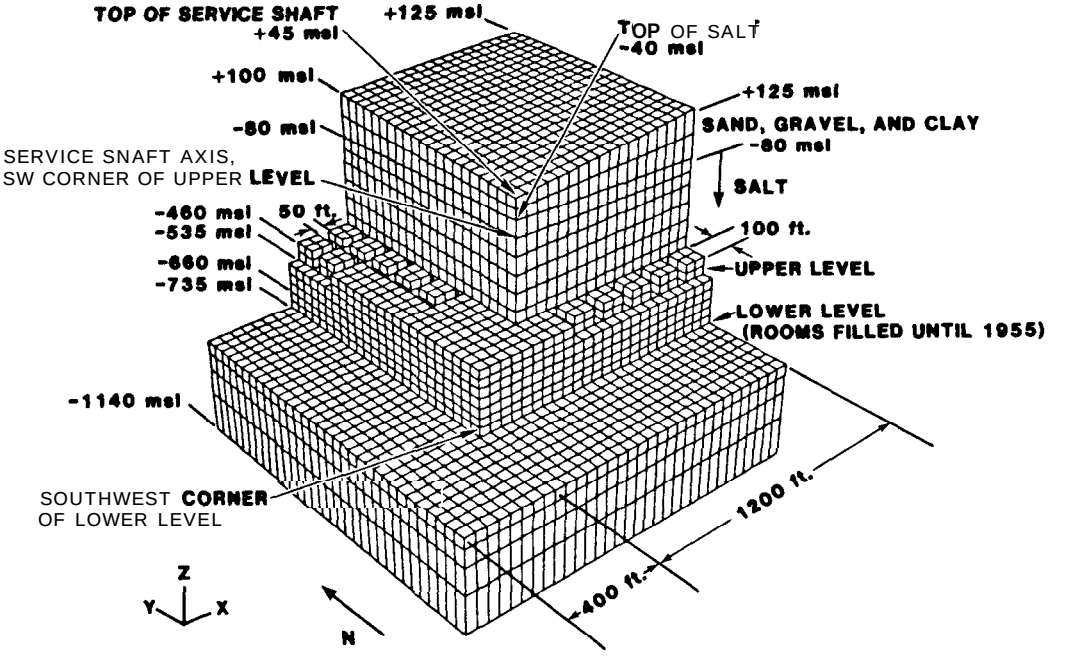

Figure 4.2. Sectioned 3-D Finite Element Model of the Weeks Island Mine and Material Adjacent to the Service Shaft

5. Calculation Results

5.1 Stress Distribution

In discussing the stress distributions on the model it should be noted that north corresponds to the Y axis of the model and east corresponds to the X axis of the model. Figure 5.1 shows the distribution of von Mises stress on the model at the beginning of the calculation which is also an elastic solution. The time of this solution is the year 1905. Von Mises stress is a scalar quantity which is proportional to the second invariant of the deviatoric stress tensor. It is used as a measure of the driving force for shear and creep deformations. The model has been sectioned on several planes and a portion of the model has been exploded vertically to allow viewing of the stresses on the pillars. It is observed in Figure 5.1 that each pillar has approximately the same stress except those around perimeter of the model. The stresses in the pillars closest to the observer are reduced slightly because these pillars are on the edge of the mine. The pillars on the north and east sides of the model (opposite the observer) have slightly reduced stresses because the symmetry boundary conditions on that side of the model double the effective width of the pillar. This condition could be changed by cutting the pillars on the north and east sides in half. This was not done because the improvement in model performance was not deemed worth the significant increase in difficulty of model generation. It should be noted that this elastic solution disturbs the stress state in the model for a limited distance.

Figure 5.2 shows the von Mises stress distribution on the model in the year **1955,** or fifty years after opening the upper level. The stresses in the pillars have dropped and the size of the disturbed zone has increased significantly due to creep. Figure 5.3 shows the von Mises stress distribution in 1955 after the room elements on the lower level of the mine have been deleted to simulate mining. A larger volume of material has been effected and the stress distribution on the lower level pillars is different than that for the upper level pillars. The lower level pillars have a yellow spot in the center of each face instead of a yellow band around the center of the pillar. Plots of σ_z and von Mises stress versus year for two specific pillars on the upper and lower layers, which are given later in Figures 5.5 and 5.6, show that the stresses in the lower level pillars are higher than in the upper level which is what would be expected. The reason for the difference in the stress distribution (yellow banding on upper level versus face-center spot on the lower level) is not completely understood. It could result from the relatively course meshing of the pillars (8 elements per pillar) or it could be caused by the relaxation of the stresses in the lower level before 1955

as a result of the upper level pillars creeping. Figure **5.4** also shows the von Mises stress distribution in the year 1955 but with the model rotated and sectioned so that the stresses on the bottom of the pillar can be seen. It should be noted that the face-centered spots of red on the bottom of most of the pillars indicate that the von Mises stresses are higher on the lower level as expected.

5.2 Pillar Stress versus Year

The vertical stress, σ_z, versus year for two pillars aligned vertically on the upper and lower levels are shown in Figure **5.5.** The location chosen for this was the third pillar diagonally from the northeast corner of the model on both the upper and lower levels. The stresses plotted were taken from the top of the upper level pillar and the bottom of the lower level pillar since those were locations where node numbers could be easily read. Figure **5.5** shows that σ_z in the upper level pillars is initially higher than in the lower level because the excavated rooms do not carry load. Between 1905 and 1955, $|\sigma_z|$ on both upper and lower levels decreases due to creep closure of the upper level. In **1955** there is a large increase in $|\sigma_z|$ on the lower level as mining of that level is simulated by removal of the room elements. $|\sigma_z|$ on both levels continues to drop with time having a slight perturbation in **1980** due to the oil fill.

Figure **5.6** shows the variation in von Mises stress versus year for the same upper and lower level pillars discussed above. The effects of mining the lower level in 1955 and oil fill in 1980 can be seen.

5.3 Calculated Underground Closure

An important element in determining the validity of these calculations is the closure of the underground rooms and the comparison of calculated closure with field data. Figure **5.7** shows vertical and horizontal closure of two vertically aligned rooms on the upper and lower level. The two rooms are adjacent to the third pillar diagonally from the northeast corner of the model on the upper and lower levels of the mine (these are the same pillars mentioned in the previous section). The impact of mining the lower level in **1955** can be seen as well as the influence of oil fill in **1980.** Horizontal closures are higher than vertical on both levels. This may, however, be an artifact of the finite element mesh since there is no node at the midpoint of the roof but there is at the midpoint of the pillar. Making the mesh fine enough to incorporate a midroof node would result in a model with eight times the number of nodes and elements as this model.

Horizontal and vertical closure rates for the upper and lower levels versus year are shown in Figure **5.8.** These curves were produced by numerical differentiation

of the the curves in Figure 5.7. Again, the impact of mining the lower level in 1955 can be seen as well as the impact of oil fill in 1980. Oil fill has a greater impact on the lower level because it is deeper and has higher oil pressure. Because the oil level is just below the roof of the upper level, oil pressures on the walls and floor of that level are relatively low.

It is interesting to note that the calculated closure rate between 1960 and 1965 is approximately 1.5 inches/year on the lower level where all the rooms are 75 feet high. The limited field data available from Morton Salt for the same period of time shows horizontal and vertical closures of approximately 0.5 inches/year in a 25-foot room. The calculated closure rate of 1.5 inches/year for a 75-foot room in this study is considerably lower than the value of approximately 3.75 inches/year calculated by (Preece, 1987) in a single pillar calculation of a 75-foot room. The single pillar study did not allow for reduction of the driving force on the pillar due to stress relaxation and redistribution. The multiple pillar model takes care of this effect naturally because it treats much more geometry. Because there is no closure data available for a 75-foot room, this discrepancy may never be adequately reconciled. However, a closure rate of 1.5 inches/year for a 75-foot room does seem reasonable when compared to the field data of 0.5 inches/year for a 25-foot room.

5.4 Calculated Surface Subsidence at the Service Shaft

The calculated surface subsidence at the Service Shaft (vertical displacement of the Service Shaft collar) is shown in Figure 5.9. The subsidence rate obtained from numerical differentiation of Figure 5.9 is shown in Figure 5.10. These two figures show a significant increase in the subsidence rate after 1955 when the lower level was mined. The calculated subsidence rate after oil fill in 1980 is approximately 0.15 inches/year. This is an order of magnitude less than that obtained from leveling data which shows a rate of approximately 1.2 inches/year between May, 1983 and April, 1986 (PB-KBB, 1986). Without more field data, i.e. leveling on deep benchmarks away from major structures, it is almost impossible to sort out this discrepancy. It may be that the subsidence of the shaft as indicated by the current leveling data is accurate which would probably mean that the constitutive models used for the rock salt and the sandy gravel overburden are not fully capturing the material behavior. It may also be that the subsidence of Service Shaft collar as indicated by current level data is not very accurate because the levels are based on benchmarks that are also subsiding (an attempt to correct the data for benchmark subsidence has been made). The fact that the Service Shaft is a major structure and may be interacting with surface materials may also have an impact. This discrepancy points to the importance of installing a high quality convergence and subsidence monitoring system at the site.

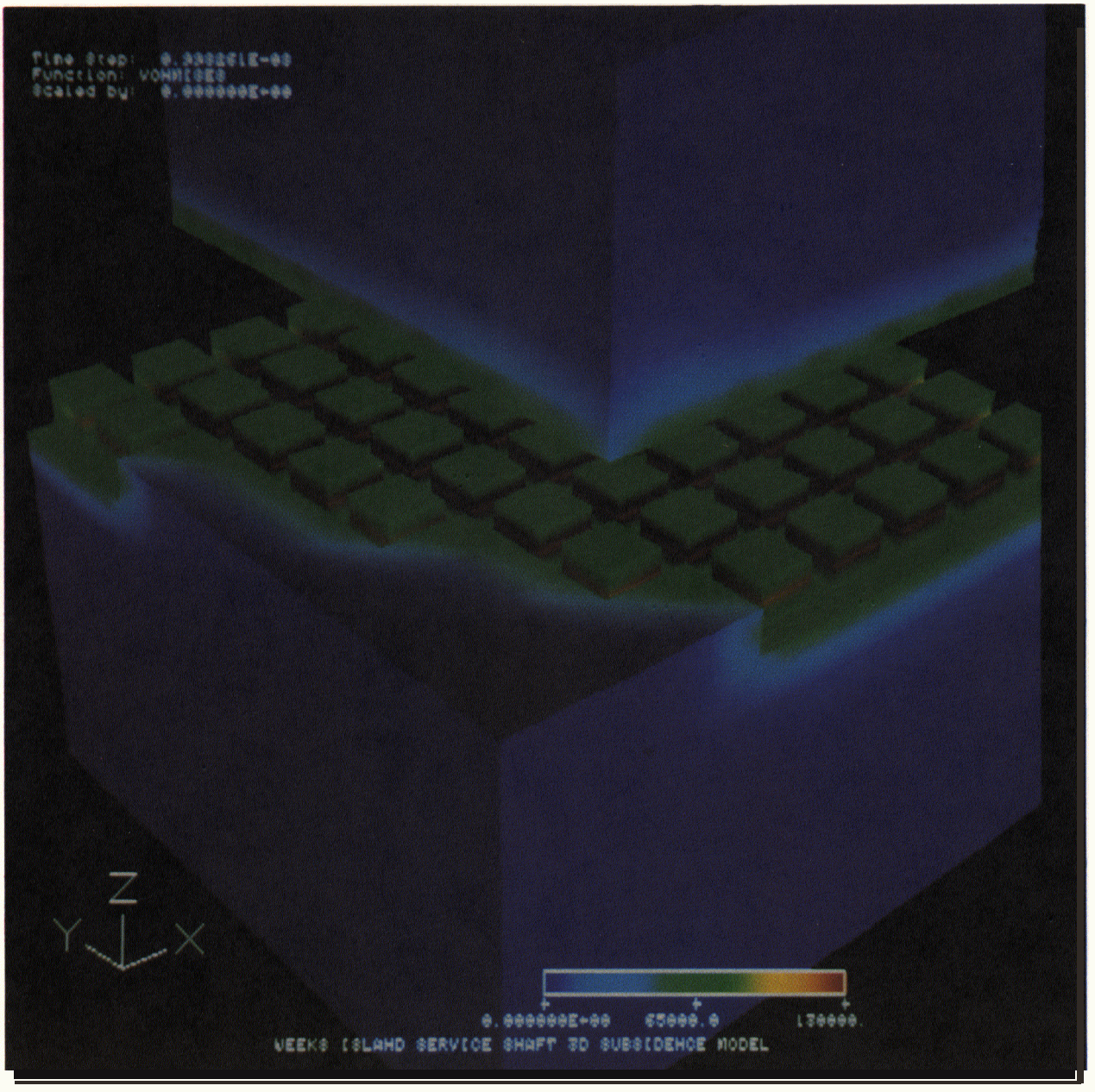

Figure **5.1.** Elastic von Mises Stress Distribution Immediately After Mining the Upper Level in **1905.**

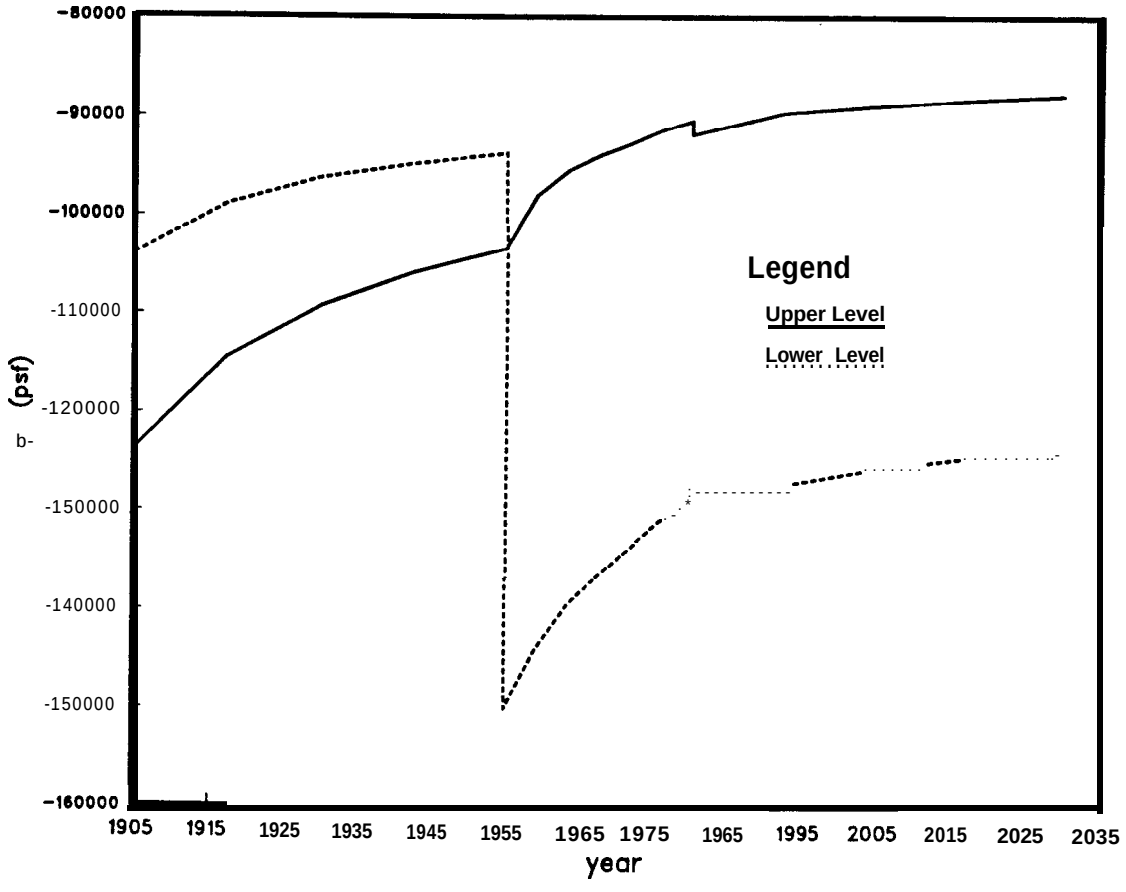

Figure 5.5. σ_z Versus Year for Two Vertically aligned Pillars on the Upper and Lower Levels. Negative Sign Stands for Compressive Stress

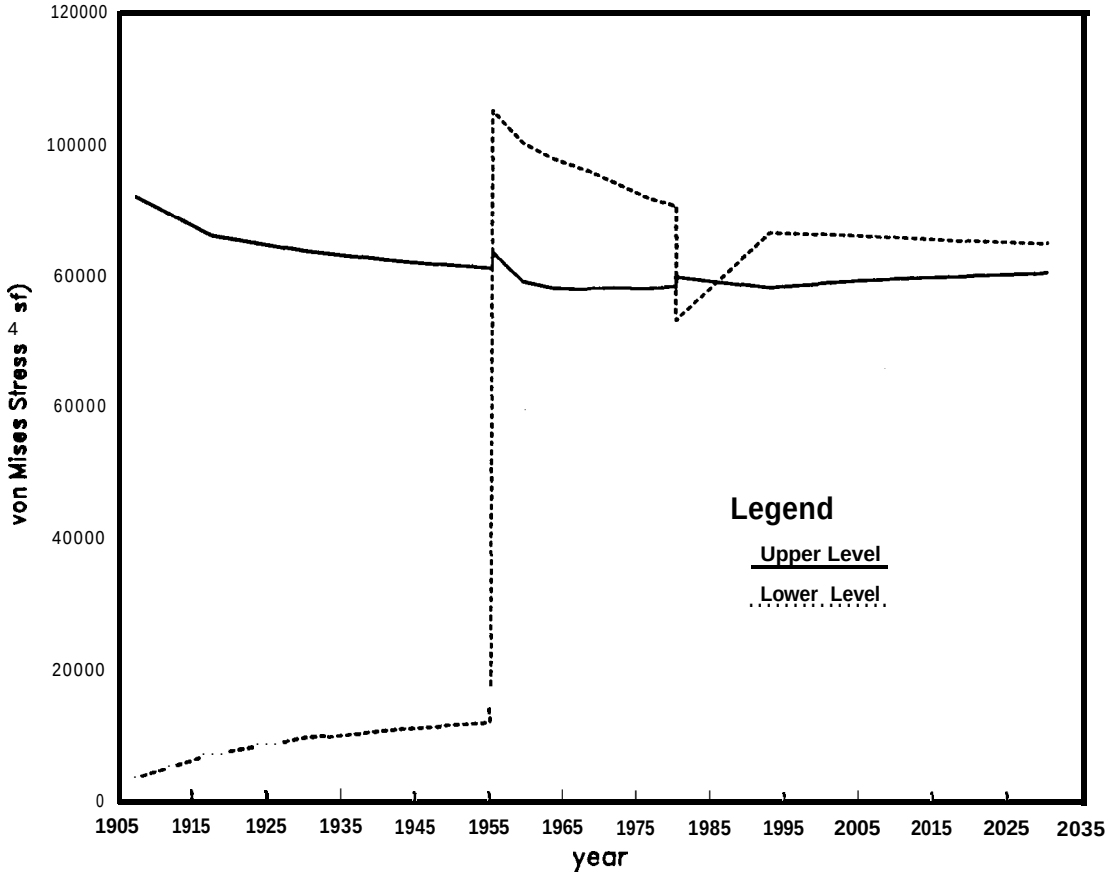

Figure 5.6. Von Mises Stress Versus Year for Two Vertically aligned Pillars on the Upper and Lower Levels.

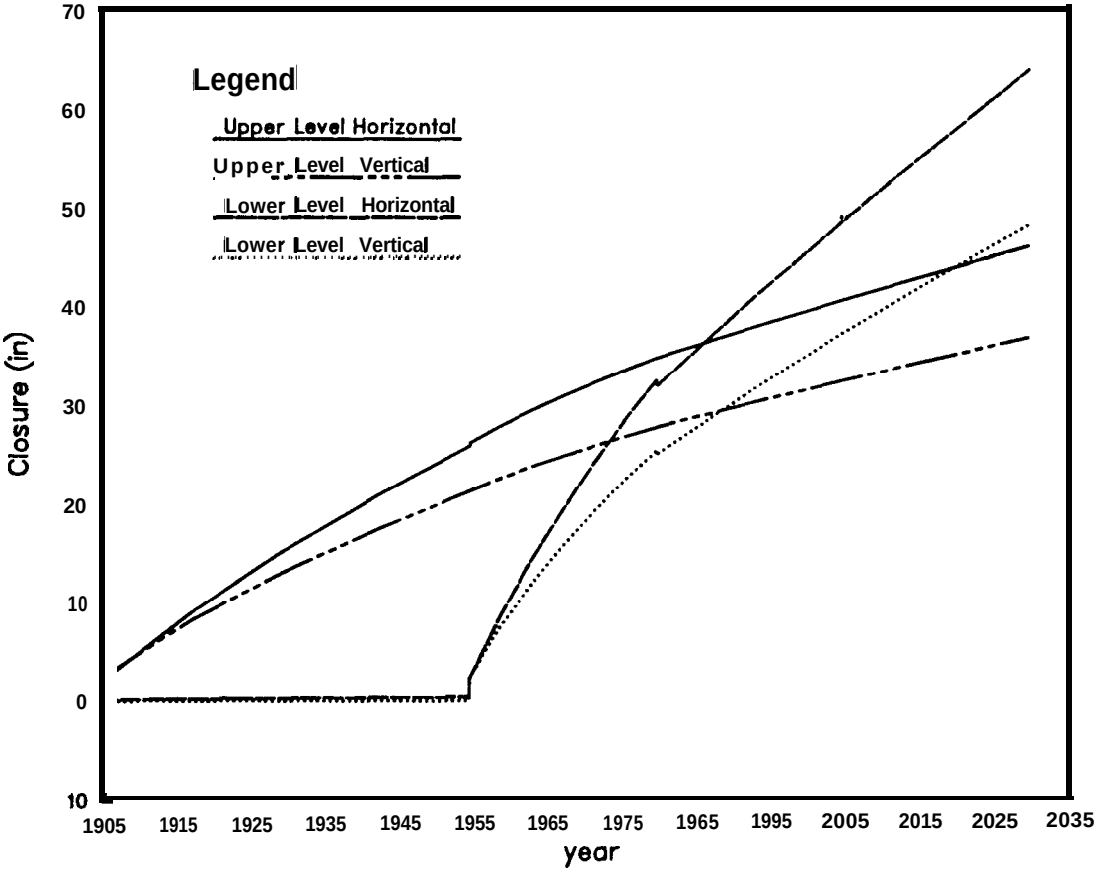

Figure 5.7. Horizontal and Vertical Closures on the Upper and Lower Levels of the Mine Versus Year.

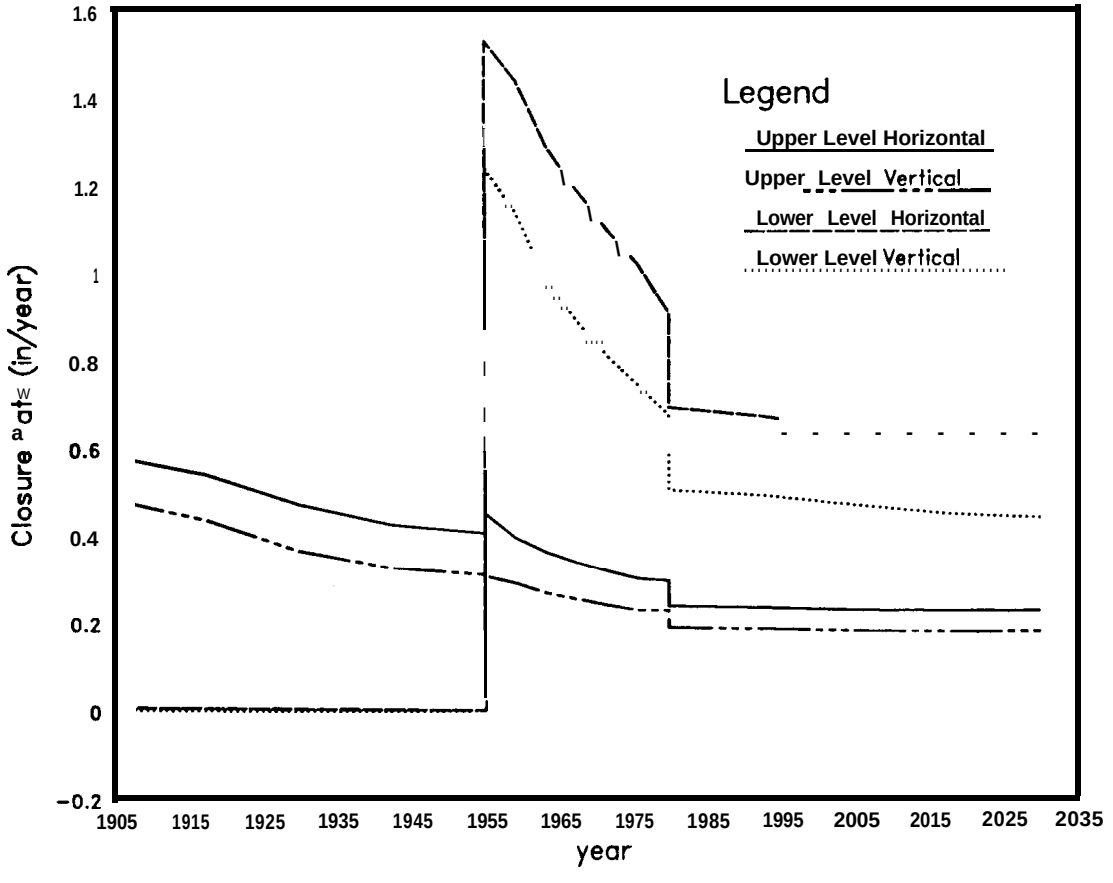

Figure 5.8. Horizontal and Vertical Closure Rates on the Upper and Lower Levels of the Mine Versus Year.

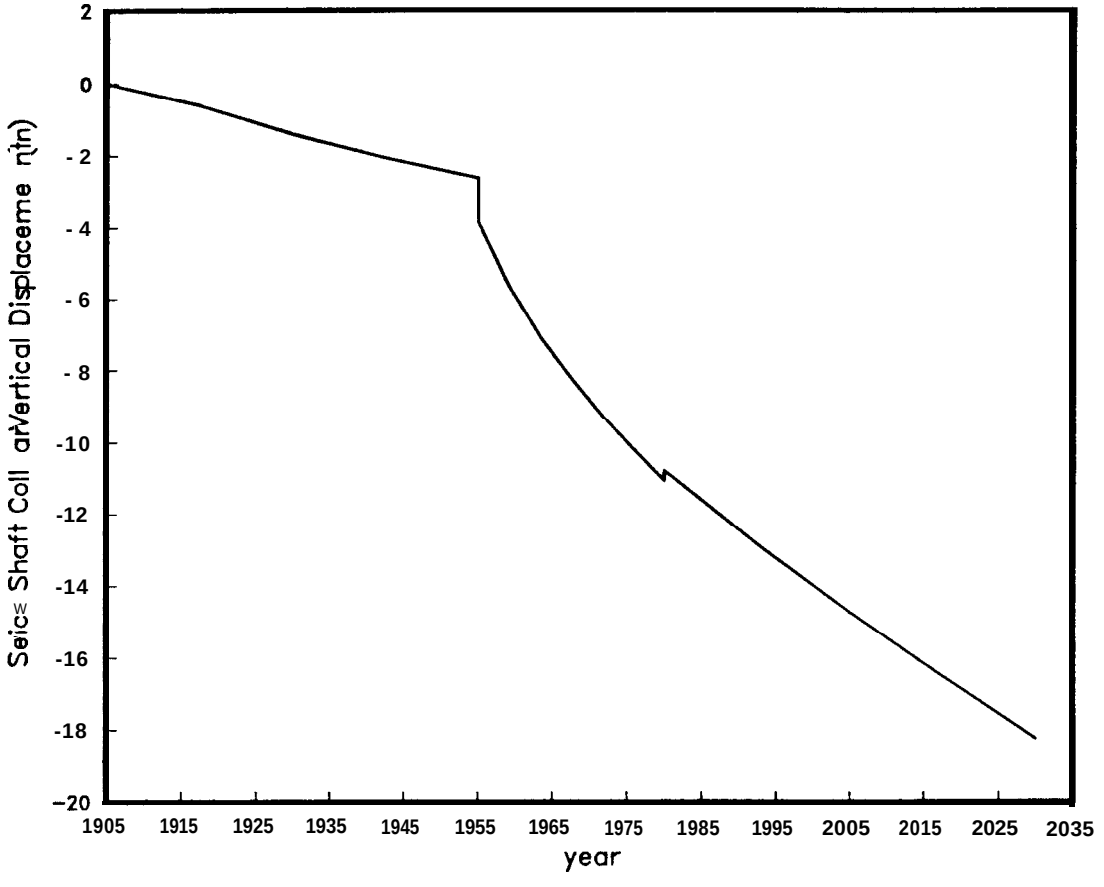

Figure 5.9. Service Shaft Collar Vertical Displacement Versus Year.

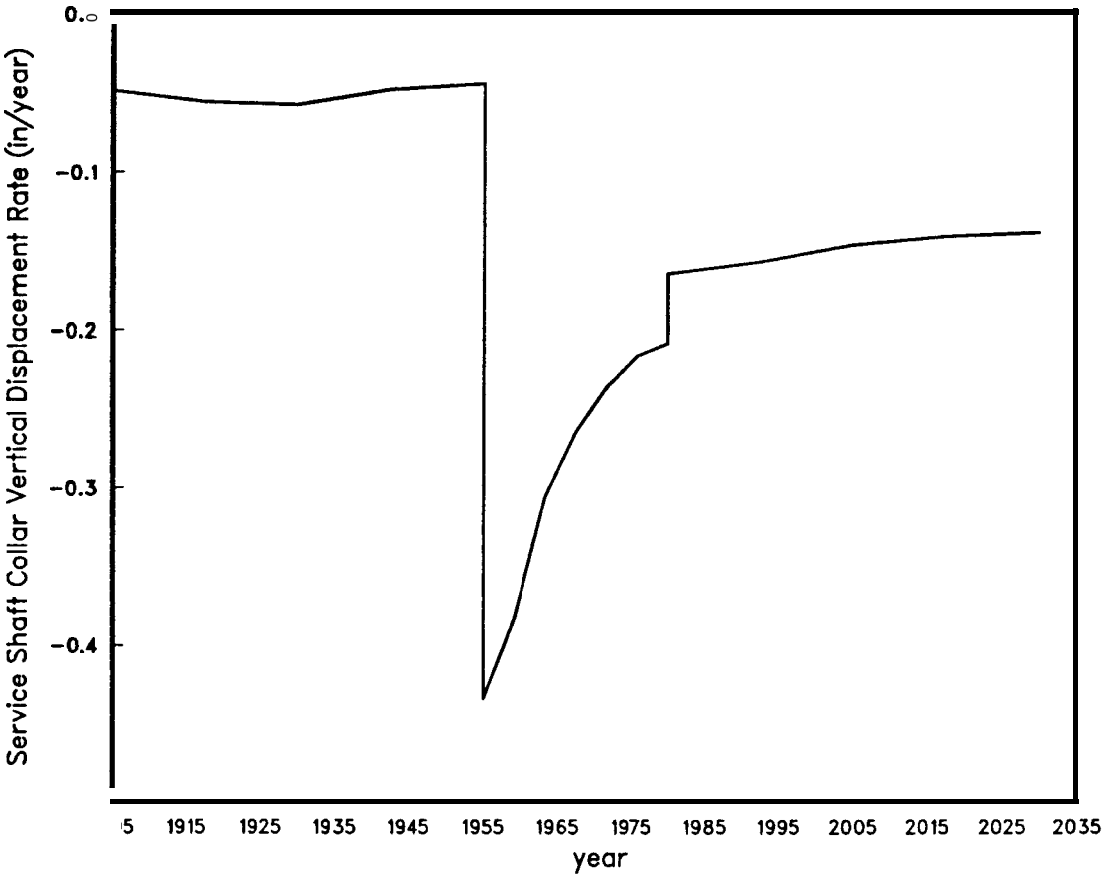

Figure 5.10. Service Shaft Collar Vertical Displacement Rate Versus Year.

6. Subsidence Induced Deformation of the Service Shaft

The movement of the Service Shaft axis is assumed to be represented by the X, Y and Z displacement of nodal points along the shaft axis from the top of the upper level to the ground surface. The location of the shaft axis on the model is shown in Figure 4.1. Figure 6.1 shows the X displacement of the shaft versus depth where 0 is at the ground surface at the shaft and -520 is at the top of the upper level. The X component of the shaft displacement seen here is almost entirely rigid body rotation. Figure 6.2 shows the Y displacement of the shaft versus depth. Again, the motion is mostly rigid body rotation though the curve for the year 2030 shows some curvature. The induced bending strain in the shaft for the year 2030 and the Y component of displacement were calculated for the upper 455 feet of the shaft. A radius of curvature of 18564 feet was calculated for this curve by fitting a circle through the coordinates of the bottom, mid and upper points on the curve. This radius of curvature and the shaft radius give a bending strain of approximately $2.5X10^{-5}$. This amount of strain could quite easily be accommodated by the shaft without significant damage.

Figure 6.3 shows Y displacement versus X displacement for three different years. This figure indicates that the shaft is tilting toward the northeast as would be expected.

The Z displacement along the axis of the shaft is shown in Figure 6.4 which shows very little axial extension or compression of the shaft. This means that the shaft is moving downward as a rigid body. The maximum axial tensile strain calculated is on the order of 10^{-4} which the shaft should be able to accommodate with a small amount of local cracking.

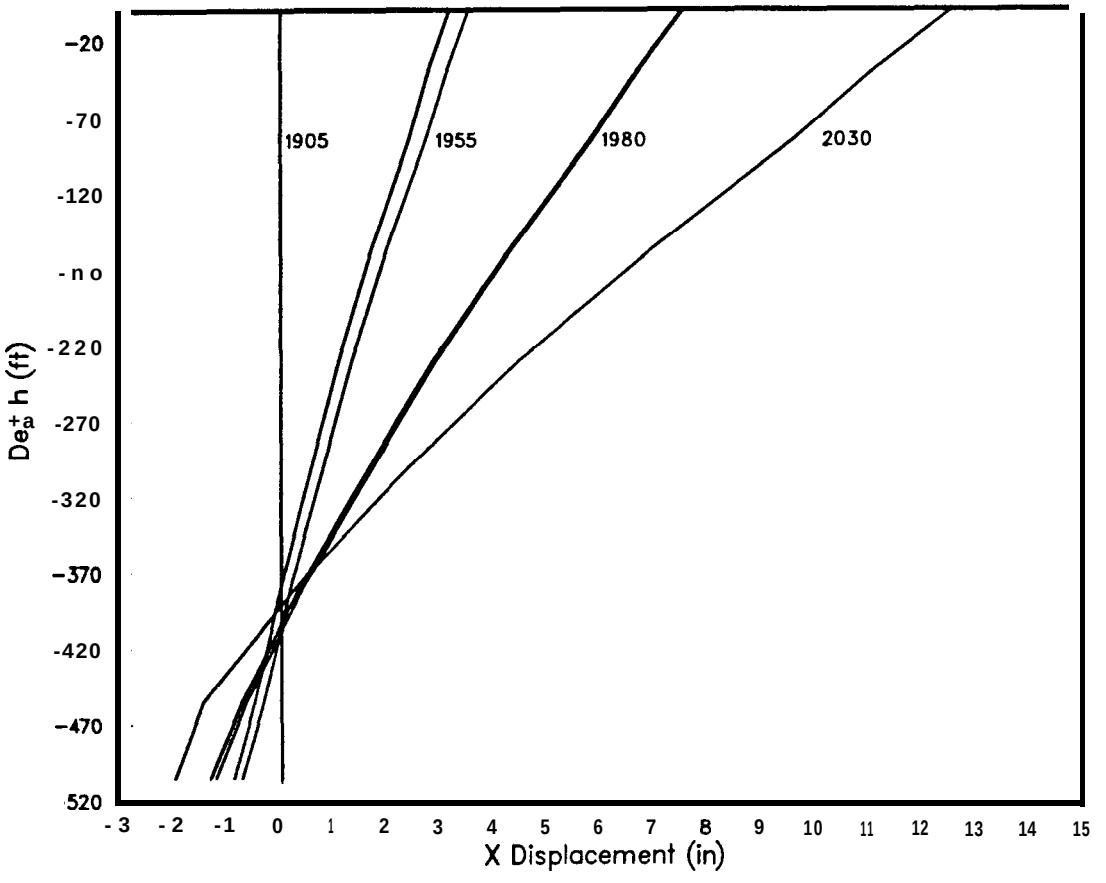

Figure 6.1. X Displacement Versus Depth Along the Axis of the Service Shaft.

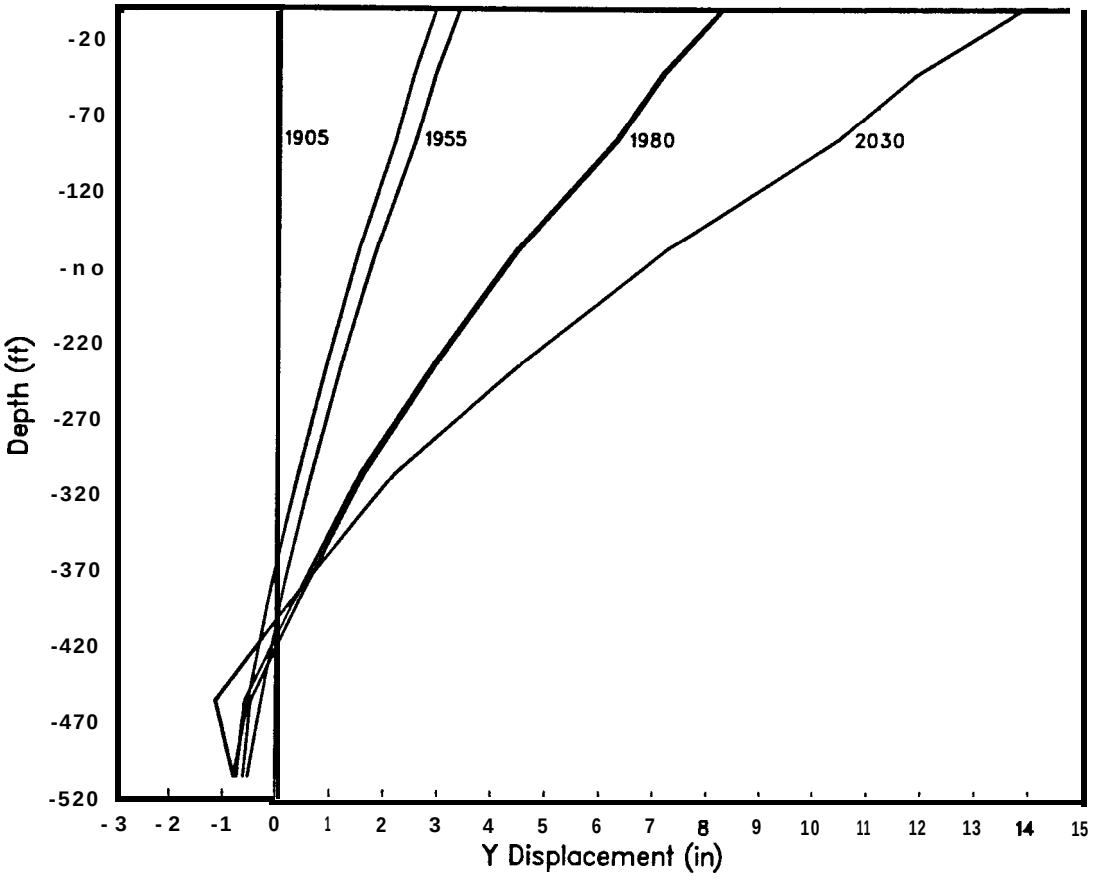

Figure 6.2. Y Displacement Versus Depth Along the Axis of the Service Shaft.

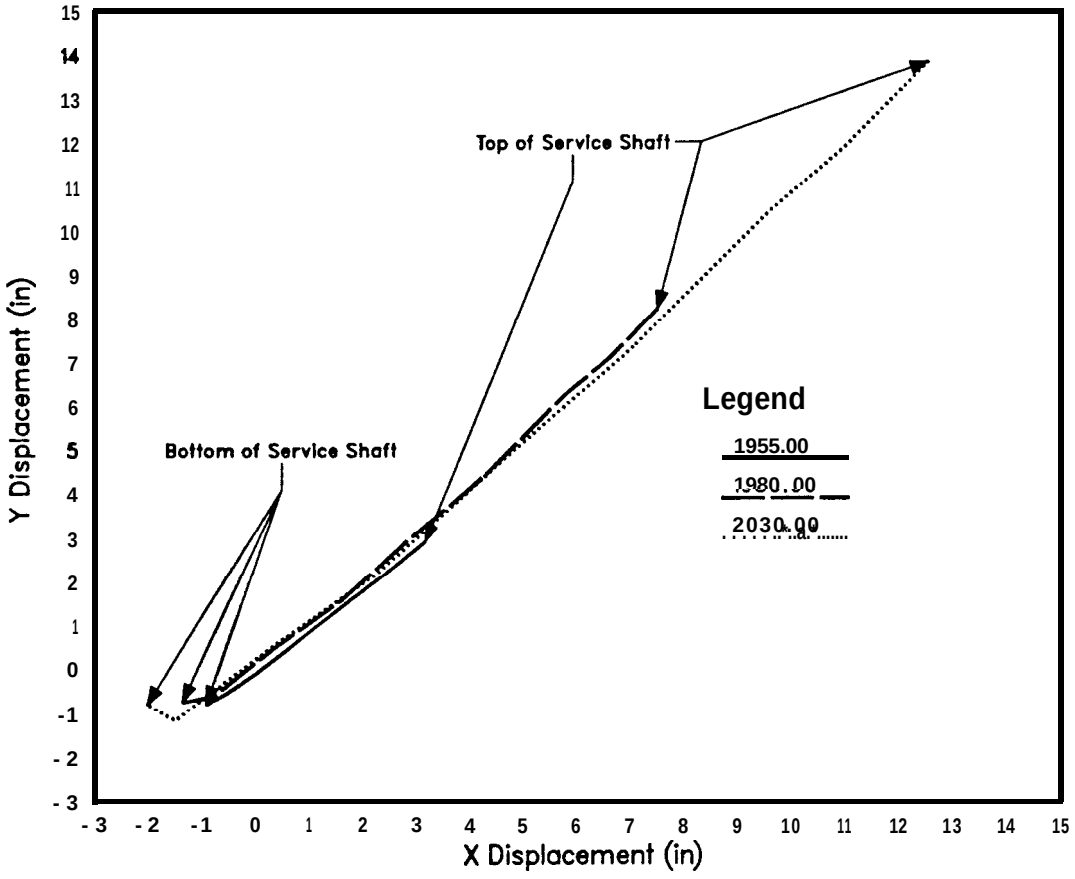

Figure 6.3. Y Displacement Versus X Displacement of the Service Shaft.

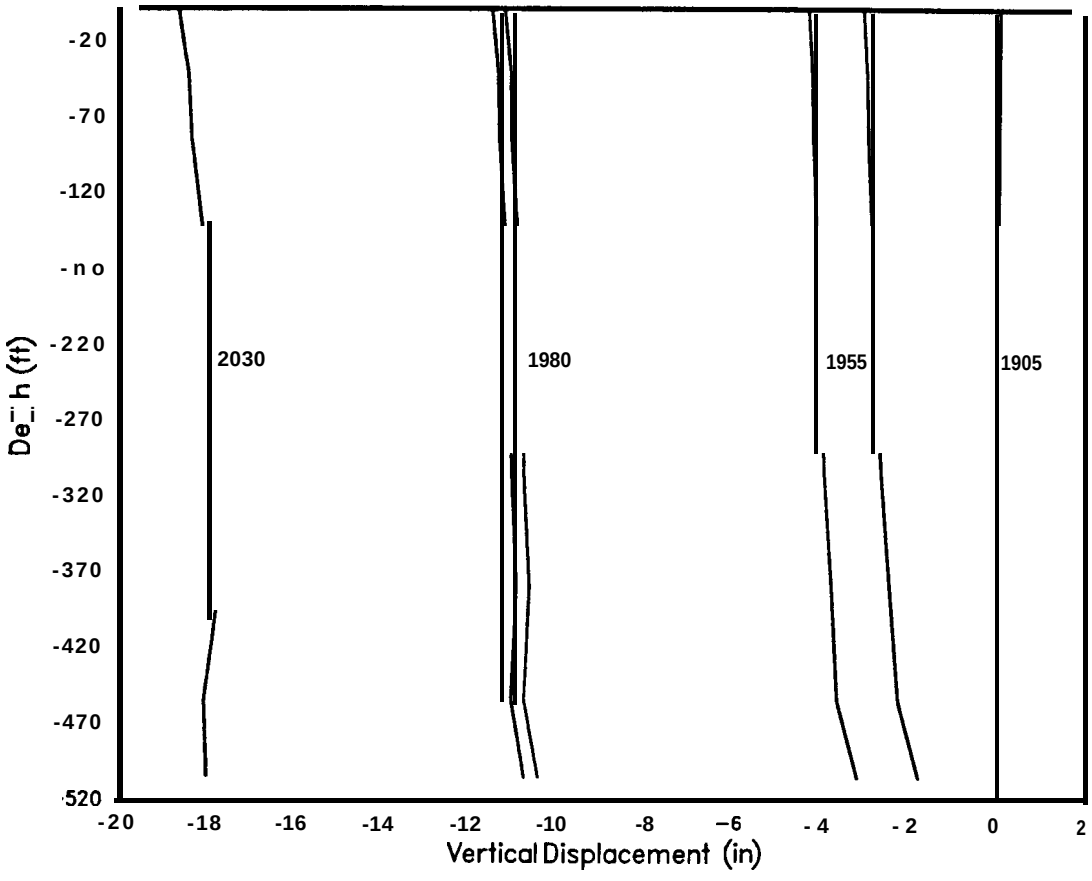

Figure 6.4. Z Displacement Versus Depth Along the Axis of the Service Shaft.

7. Conclusions

A 3-D finite element creep calculation which treats the southwest corner of the Weeks Island mine has been completed. The model was created to examine the movement of the Service Shaft resulting from subsidence which is caused by creep closure of the bi-level room-and-pillar salt mine. The model treats the geometry relatively well, including 54 pillars on the upper level and 64 pillars on the lower level. Each pillar contains eight finite elements and the entire model contains 18,916 finite elements and 21,780 nodal points.

Movement of the shaft has been measured over the past few years using survey levels. The major concern with the shaft is whether movement will somehow result in rupture. Rupture of the shaft above the interface between the salt and overburden could result in flooding of the underground works including the drawdown pumping facilities.

This calculation'shows movement of the shaft as the field data indicates, but the movement seen is dominated by rigid body rotation to the northeast and translation downward. The rigid body displacement of the shaft seen in these calculations results in very little deformation of the shaft. The deformations calculated in terms of bending and axial strain are small enough to be accommodated by the shaft without rupture.

The calculated vertical and horizontal closure rates of the 75-foot rooms in the mine are reasonable when compared to the limited Morton field obtained from a 25-foot high room. This gives some confidence in the creep model being employed. A discrepancy exists in this calculation between the measured and calculated vertical displacement rate at the Service Shaft collar, the measured rate being approximately a factor of ten higher than the calculated rate. The obtaining of higher quality field data and performing more calculations should result in correction of this discrepancy. Whether the correction of this discrepancy will have any effect on the calculated deformation of the Service Shaft is not known at this time.

This study of the Service Shaft is encouraging because it indicates that the shaft is probably stable. The results of this study are also corroborated by the fact that the Service Shaft was completed in 1905 and has been in operation since. The subsidence rate due to the oil-filled mine is less now than when the mine was empty because the oil pressure reduces the creep closure rate of the mine and consequently the subsidence rate. Oil fill, then, should reduce the movement of the shaft, as

these calculations indicate. However, Morton Salt is continuing to mine at the site with current operations being northwest of the Service Shaft and tentative plans for mining below the oil storage area. The new mining will definitely have an effect on the subsidence induced movement of the shaft. Whether these movements will continue to be dominated by rigid body motion can only be determined by more calculations.

REFERENCES

Acres International

Weeks Island Mine Gwtechnical Study, Contract FEA-1251-75, Acres International Inc., Buffalo, NY, November 1977.

Acres International

Additional Gwtechnical Studies Strategic *Petroleum Reserve (SPR),* SAND86-7181, Sandia National Laboratories Contractor Report, Albuquerque, NM, December 1986.

Arguello, J. G., D. E. Munson and D. S. Preece

Preliminary *Results of the Three-Dimensional* Modeling *of the WIPP Room D Excavation Sequence,* Proceedings of 28th U. S. Symposium on Rock Mechanics, Tucson, AZ, June 1987

Biffle, **J. H.**

JAC - A Two-Dimensional Finite *Element Computer Program for the Non-Linear* Quasistatic *Response* of *Solids With the Conjugate Gradient Method,* SAND81-0998, Sandia National Laboratories, Albuquerque, NM, April 1984.

Biffle, J. H.

JAC3D Preliminary User's *Manual,* Internal Documentation, Sandia National Laboratories, Albuquerque, NM, 1986.

Branstetter, L. J., and D. S. Preece

Numerical Studies *of Laboratory Triaxial Creep Tests,* Proceedings of 24th U. S. Symposium on Rock Mechanics, Texas A & M University, College Station, TX, June 1983.

Hansen, F. D.

Quasi-Static Strength and Deformational Characteristics of Salt and Other Rock From the Weeks Island Mine, RE/SPEC Inc., Rapid City, SD, October 1977.

Hilton, P. D., S. E. Benzley and M. **H. Gubbels**

Structural Analysis *of Weeks Island Mine/Petroleum Repository,* SAND740595, Sandia National Laboratories, Albuquerque, NM, August 1979.

Herrmann, W. and H. S. Lauson

Analysis *of Creep Data for Various Natural Rock Salts,* SAND81-2567, Sandia National Laboratories, Albuquerque, NM, December 1981.

Krieg, **R. D., C. M. Stone and S. W. Key**
Comparisons of the Structural Behavior of Three Storage Room Designs for the WIPP Project, SAND80-1629, Sandia National Laboratories, Albuquerque, NM, 1981.

Krieg, R. D.
Implementation of Creep Equations for Metal Into a Finite Element Computer Program, Computer Methods for Nonlinear Solids and Structural Mechanics, ASME, AMD-Vol54, pp133-144, 1983.

Morgan, H. S., R. D. Krieg and R. V. Matalucci
Comparative Analysis of Nine Structural Codes Used in the Second WIPP Benchmurk Problem, SAND81-1389, Sandia National Laboratories, November 1981.

Morgan, H. S., C. M. Stone and R. D. Krieg
The Use of Field Data to Evaluate and Improve Response Models for the Waste Isolation Pilot Plant (WIPP), 26th U. S. Symposium on Rock Mechanics, Rapid City, SD, June 1985.

Morgan, H. S., C. M. Stone and R. D. Krieg
An Evaluation of WIPP Structural Modeling Capabilities Based on Comparisons With South Drift Data, SAND85-0323, Sandia National Laboratories, Albuquerque, NM, 1986.

Morgan, H. S.
Estimate of the Time Needed for TRU Storage Rooms to Close, Sandia Memorandum to D. E. Munson, Sandia National Laboratories, Albuquerque, NM, June 2, 1987.

PB-KBB Inc.
Weeks Island Subsidence and Convergence Monitoring Programs PB-KBB Inc., Houston, TX, November, 1986.

PDA Engineering
PATRAN Users Guide PDA Engineering Software Products Division, Santa Ana, Calif., 1987

Preece, D. S. and W. R. Wawersik
Leached Salt Cavern Design Using a Fracture Criterion for Rock Salt, Proceedings of the 25th U. S. Symposium on Rock Mechanics, Northwestern University, Evanston, Illinois, June 1984.

Preece, D. S. and R. D. Krieg
Finite *Element Study of Working Level* Separation *at the Weeks Island Salt Dome,* SAND84-1021, Sandia National Laboratories, Albuquerque, NM, July 1984.

Preece, D. S. and **H. J.** Sutherland
Physical and Numerical *Simulations of Fluid-Filled* Cavities in *a Creeping Material,* SAND86-0694, Sandia National Laboratories, Albuquerque, NM, May 1986.

Preece, D. S.
Calculation of Creep Induced Volume Reduction of the Weeks Island SPR Facility Using *3-D* Finite *Element Methods* SAND87-1694, Sandia National Laboratories, Albuquerque, NM, September, 1987.

Stone, C. M., R. D. Krieg and **Z. E.** Beisinger
SANCHO - A Finite *Element Computer Program for the* Quasistatic, Large *Deformation, Inelastic Response of* Two-Dimensional Solids, SAND84-2618, Sandia National Laboratories, Albuquerque, NM, April 1985.

Wawersik, W. R., and D. **H. Zeuch**
Creep and Creep Modeling *of Three Domal Salts - A Comprehensive Update,* SAND84-0568, Sandia National Laboratories, Albuquerque, NM, May 1984.

Distribution:

US DOE SPR PMO (10)
900 Commerce Road East
New Orleans, LA 70123
E. E. Chapple, PR-63 (5)
L. J. Rousseau, PR-63 (1)
J. W. Smollen, PR-63 (2)
TDCS (2)

US Department of Energy (1)
Strategic Petroleum Reserve
1000 Independence Avenue SW
Washington, DC 20585
D. Smith

US Department of Energy (1)
Oak Ridge Operations Office
P. 0. Box E
Oak Ridge, TN 37831
J. Milloway

Acres International Corporation (3)
Suite 1000 Liberty Building
424 Main Street
Buffalo, NY 14202-3592
Bill Lamb
Stewart Thompson
Tom Magorian

Aerospace Corporation (2)
800 Commerce Road West, Suite 300
New Orleans, LA 70123
R. Merkle

PB/KBB (4)
850 South Clear-view Parkway
New Orleans, LA 70123
H. Lombard (4)

PB/KBB (2)
Weeks Island
P. 0. Box 434
New Iberia, LA 70560
C. Chabannes (2)

Boeing Petroleum Services (5)
850 South Clearview Parkway
New Orleans, LA 70123
J. Schmedeman (4)
K. Mills

Walk-Haydel & Associates, Inc. (3)
600 Carondelet St.
New Orleans, LA 70130
Cary Trochesset
John Rabai
J.Mayes

Dr. S. E. Benzley
Civil Engineering Dept. 368CB
Brigham Young University
Provo, Utah 84602

Dr. C. H. Conley
School of Civil and Environmental Engineering
Hollister Hall
Cornell University
Ithaca, NY 14853

Sandia Internal:

1510 J. W. Nunziato
1520 C. W. Peterson
1521 R. D. Krieg
1521 H. S. Morgan
1530 L. W. Davison
1550 R. C. Maydew
3141-1 S. A. Landenberger (5)
3154-4 C. Dalin, For: DOE/TIC (28)
3151 W. L. Garner (3)
6000 D. L. Hartley
6200 V. L. Dugan
6230 W. C. Luth
6232 W. R. Wawersik
6232 D. H. Zeuch
6250 B. W. Marshall
6257 J. K. Linn (10)
6257 J. L. Todd
6257 J. T. Neal
6258 D. S. Preece (20)
6332 L. D. Tyler
6332 J. G. Arguello
8024 P. W. Dean

☆ U S GOVERNMENT PRINTING OFFICE 1987--573-049/61028